GEOPHYSICAL RESEARCH LETTERS, VOL. 25, NO. 2, PAGES 183-186, January 15, 1998

Upper ocean velocities in the Beaufort Gyre

A. J. Plueddemann[1], R. Krishfield[1], T. Takizawa[2]
K. Hatakeyama[2] and S. Honjo[1]

Abstract. A 23 month time series of upper ocean velocities in the Beaufort Gyre was obtained from an autonomous drifting buoy equipped with an Acoustic Doppler Current Profiler. The buoy was deployed in the Beaufort Sea and drifted over the Canada Basin, Chukchi Shelf, and Chukchi Plateau. Time-evolving spectral analysis was used to examine velocity variability in three frequency bands: an eddy band (2–5 day periods), a diurnal band, and a semidiurnal band. The eddy band and the semidiurnal band dominated the horizontal kinetic energy. Although eddy energy was clearly confined to the Beaufort Sea and Canada basin, eddies were found further to the south and west than in previous observations. The semidiurnal band was dominated by near-inertial motions with amplitude that varied seasonally (largest in late summer and smallest in late winter). Diurnal tides were weak (< 1 cm s^{-1}) except over a shallow portion of the Chukchi Shelf.

Introduction

Despite decades of exploration, the velocity field beneath the pack ice of the Arctic Ocean is not well described. A network of satellite-tracked drifting buoys frozen into the ice provides an assessment of surface motion [*Colony and Thorndike*, 1984], but subsurface velocities are not observed. Subsurface velocities have been measured from ice camps, but the most comprehensive experiments are often of short duration [*CEAREX Drift Group*, 1990; *LeadEx Group*, 1993]. In this paper we report the results of long-duration, subsurface velocity measurements from a drifting buoy deployed in the Beaufort Gyre.

In April 1992 an autonomous drifting buoy was frozen into the Arctic pack ice about 150 miles north of Prudhoe Bay, Alaska. The buoy was one in a series of Ice-Ocean Environmental Buoys (IOEBs) designed for long-term measurement of meteorological and oceanographic variables in the Arctic [*Krishfield et al.*, 1993; *Honjo et al.*, 1995]. The IOEB consisted of a flotation collar and electronics package at the surface connected mechanically and electronically to a string of instruments suspended below. The surface element contained meteorological sensors, ice sensors, and two antennas for satellite communications. Below the surface was a string of sensors for measurement of water properties, currents, and particle flux. Sensor data were collected and processed by a controller in the surface electronics package and then transmitted to Argos satellites.

[1]Woods Hole Oceanographic Institution, Woods Hole, Massachusetts, USA 02543
[2]Japan Marine Science and Technology Center, Yokosuka, Japan 237

Paper number 97GL53638.
0094-8534/98/97GL-53638$05.00

The IOEB was deployed from the Arctic Leads Experiment ice camp in the Beaufort Sea [*LeadEx Group*, 1993] and tracked for 4 years while executing a broad, anticyclonic arc centered on the Canada Basin. The long-term drift was consistent with the mean pattern of ice motion estimated from satellite-tracked drifters [*Colony and Thorndike*, 1984] and indicated that the buoy was captured within the wind-driven Beaufort Gyre [*Pfirman et al.*, 1997]. During most of the first two years, the IOEB transmitted data from meteorological sensors, a current profiler, and a transmissometer-fluorometer logger. Shorter duration time series were obtained from ice thermistor strings and subsurface conductivity-temperature loggers [*Honjo et al.*, 1995].

This paper focuses on data transmitted from the current profiler during the first two years. The IOEB traversed several distinct geographic regions during this period (Fig. 1).

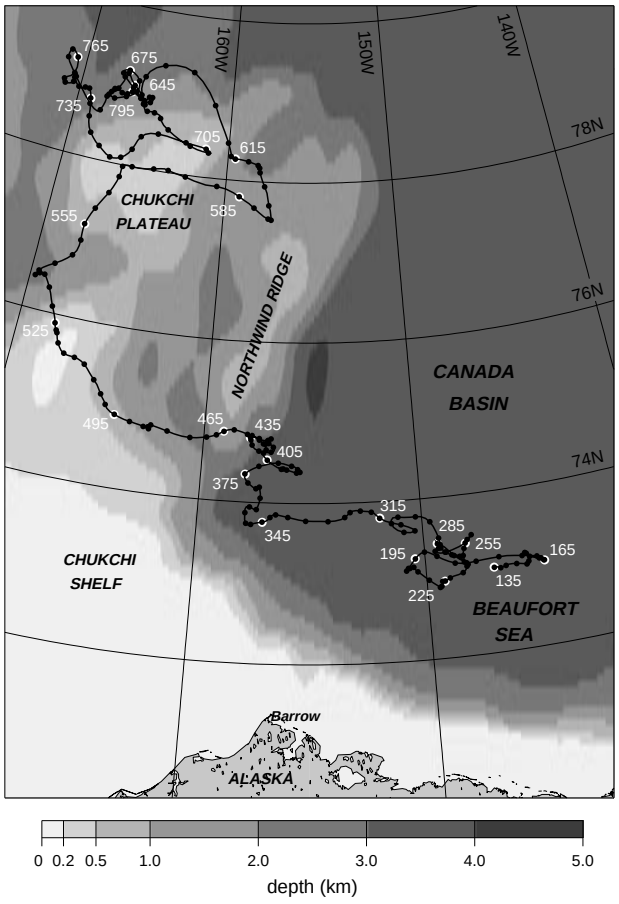

Figure 1. Drift track of the IOEB superimposed on bathymetry. The track has been smoothed over 6 days prior to plotting. Symbols are plotted every 3 days. Annotated symbols give the year day starting from 14 May 1992 (day 135).

The buoy remained in the northwest Beaufort Sea for about 2 months after deployment. The drift during the next 6 months was westward across the Canada Basin and past the southern foot of the Northwind Ridge. During the next 2 months the drift track crossed the northern Chukchi Shelf, passing over the shallow, northward projection of the shelf near 76° N, 168° W. The buoy partially crossed the Chukchi Plateau several times during the next 7 months, finally settling on its westward slope during the last 2 months.

Methods

An RD Instruments 150 kHz Acoustic Doppler Current Profiler (ADCP) was suspended at 8 m depth below the surface with the transducers pointing downwards. Forty acoustic transmissions were averaged within the ADCP to produce an ensemble every 15 min. Forty depth cells of 8 m length were recorded for each ensemble, giving a nominal profiling range of 26 to 338 m depth. Because the data produced by the ADCP far exceeded the transmission capacity of the Argos system, a Data Processing Module (DPM) was developed to reduce the data [*Plueddemann et al.*, 1992]. The DPM collected 15 min ensembles from the ADCP, averaged the velocities over 2 hours in time and 3 bins in depth, and combined the ancillary data into a small number of quality flags.

The DPM provided velocities for the first 10 averaged depth bins to the IOEB controller in two separate data streams, one containing even numbered bins and the other containing odd bins. The two data streams were transmitted to Argos on separate channels. Unfortunately, the channel transmitting the even bin data failed after about one month. The data presented here are from the odd bins, with bin centers at 58, 106, 154, 202 and 250 m depth. An estimate of velocity at the surface was made from the buoy positions. This drift velocity was smoothed with a 6 hour triangle filter, interpolated to 2 hours, and then removed from the ADCP data in post-processing to yield absolute subsurface velocities. The absolute velocities were accurate to only a few cm s^{-1} due to uncertainty in the Argos positions. The velocity precision was limited by noise in the 2 hour ADCP velocities, estimated to be about 0.5 cm s^{-1}.

Data were processed for a 23 month period from 6 May 1992 to 29 March 1994 (days are subsequently referred to by sequential year day from 135 [14 May 1996] to 810 [20 March 1994]). Frequency spectra for the surface and each depth bin were estimated from successive 15 day sections, stepped forward in time by 3 days. A frequency band dominated by eddy variability (2–5 day periods, subsequently called the "eddy band") was identified in the spectra and isolated by frequency domain filtering. Variability in the eddy band resulted from the buoy passing over subsurface eddies which were moving slowly relative to the ice. The period of this variability was determined by the size of the eddies and the speed of encounter. Eddies in the Beaufort Sea and Canada Basin have diameters of order 20 km [*Manley and Hunkins*, 1985; *D'Asaro*, 1988]. The short-term (e.g., weekly) buoy drift speed relative to 250 m depth was typically 5 cm s^{-1}, and seldom greater than 10 cm s^{-1}. A 20 km eddy encountered at speeds of 5–10 cm s^{-1} would result in temporal variability at 2–5 day periods.

A semidiurnal band (11.6-12.8 hour periods, subsequently called the "inertial band") was also isolated by frequency domain filtering. Attempts to separate near-inertial motion and semidiurnal tidal constituents using complex demodulation [*Pease et al.*, 1995] were not successful. However, results from the high-resolution tidal model of *Kowalik and Proshutinsky* [1993; 1994] provided a practical solution. The predicted S_2 and M_2 tides along the drift track were seldom as large as the ADCP noise level (0.5 cm s^{-1}). This implied that nearly all of the observed semidiurnal energy was due to near-inertial motion (the inertial period varied from 12.55 to 12.21 hours along the track). The exceptions were when the buoy passed over the shallowest portions of the Chukchi Shelf and Plateau, where the predicted S_2 and M_2 amplitudes were between 0.5 and 1.0 cm s^{-1}. Inertial-band amplitudes in these regions were interpreted with caution.

The time-varying amplitude of the diurnal tidal constituents O_1 and K_1 were estimated using complex demodulation [*McPhee*, 1980a; *Pease et al.*, 1995]. Clockwise and counter-clockwise rotating components for the two constituents were determined from the same 15 day segments used for spectral estimation.

Results

The time-evolving frequency spectrum (Fig. 2) showed distinct temporal variability in several frequency bands. Periodic increases and decreases in energy were seen in the inertial band, with relative maxima near days 250 and 600. The diurnal band showed intermittent, weak energy maxima. Low-frequency energy dominated the early part of the record, decreased dramatically when the buoy left the Canada Basin (day 405), and then increased slightly as the buoy entered the Chukchi Plateau region (day 540). Spectral levels at all frequencies showed a minimum as the buoy crossed the southern foot of the Northwind Ridge and approached the Chukchi Shelf (days 420–500). Variability in the inertial, diurnal, and eddy bands are discussed in more detail below.

The principal characteristic of the inertial-band amplitude (Fig. 3a) was seasonal variability, presumably due to seasonal changes in the pack ice [*McPhee*, 1980b]. Fragmented summer ice supports very little internal stress. As a result, surface winds generate inertial currents and downward propagating near-inertial waves analogous to those in the open ocean. In winter much of the wind stress is converted to internal stress in the tightly packed ice and inertial currents are weak or absent. The air temperature from the IOEB (Fig. 3b) illustrates the change of season during the drift. Inertial amplitudes were largest in late summer and smallest in late winter.

The buoy spent the first summer in the Canada Basin where the inertial-band amplitude peaked at 3–6 cm s^{-1} in August and September (days 214–274). Amplitudes decreased to about 2 cm s^{-1} by mid October (day 290). During the first winter the amplitudes were near the noise level of the observations (0.5 cm s^{-1}). A peak of about 2 cm s^{-1} was seen in early June (day 520) while the buoy was over the shallowest part of the Chukchi Shelf. It is likely that this peak was due to enhanced semidiurnal tides [*Kowalik and Proshutinsky*, 1994] rather than inertial currents.

The second summer was spent near the Chukchi Plateau. Amplitudes of 4–11 cm s^{-1} were seen from July through September (days 550–630). Interestingly, the largest amplitudes were not directly over the plateau (days 555–580),

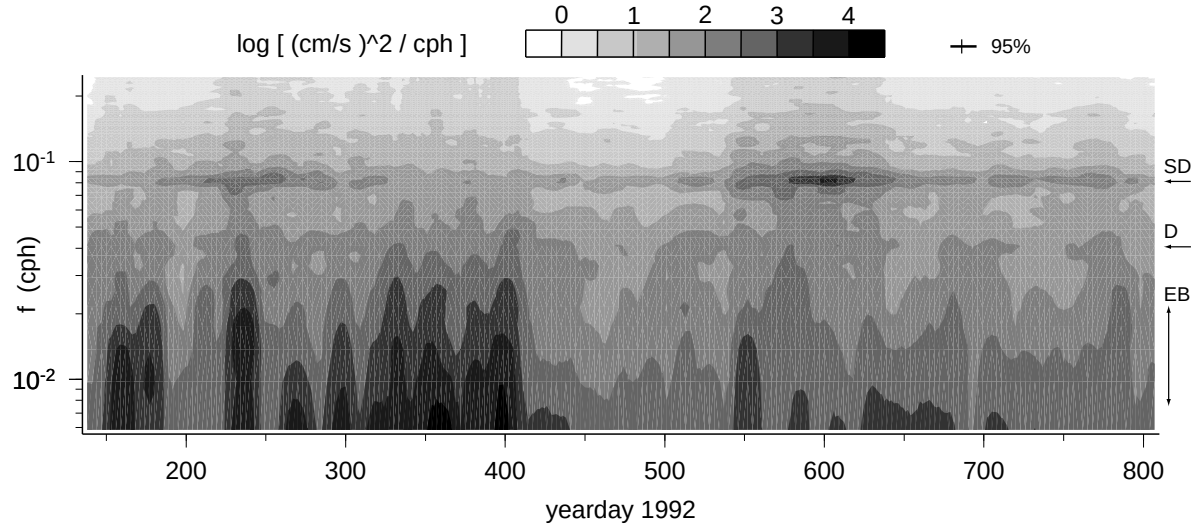

Figure 2. Time-evolving frequency spectrum of velocity. Successive spectral estimates are from 15 day sections, computed at 3 day intervals and averaged over the 5 ADCP depth bins (58–250 m). The locations of the semidiurnal (SD) and diurnal (D) frequencies are shown to the right of the figure along with the width of the eddy band (EB).

but over the northeast plateau slope (day 585) and over the trough separating the northern Chukchi Plateau from the Northwind Ridge (day 605). Most of the second winter was spent over the northwest plateau slope, although the plateau was also partially crossed (days 680–735). As observed in the first year, inertial-band amplitudes decreased to 2 cm s^{-1} by mid October (day 650), but unlike the first winter amplitudes remained at 1–2 cm s^{-1} from October to March (days 650–810). The 2.5 cm s^{-1} peak observed over the shallow, northern tip of the plateau (day, 710) could have been due to the M_2 tide, but predicted semidiurnal tidal amplitudes were less than 0.5 cm s^{-1} elsewhere. Inertial energy could have been sustained during the winter if the energy source were oscillatory tidal currents interacting with bottom topography [*Bell*, 1975] rather than surface winds.

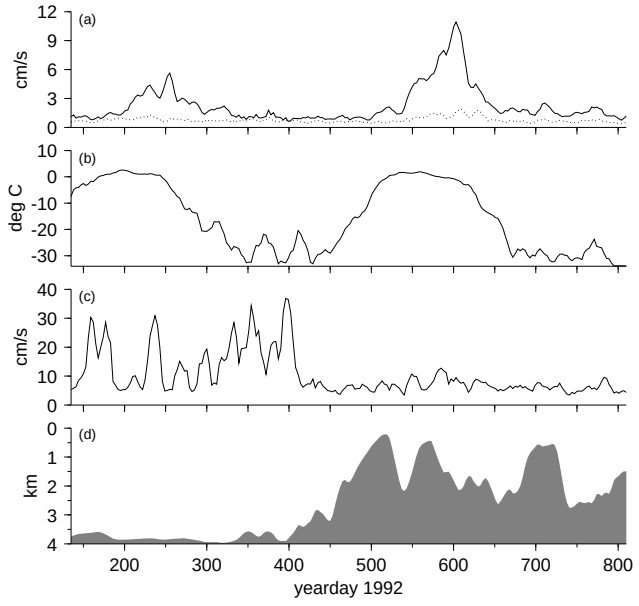

Figure 3. Inertial-band and eddy-band amplitudes. (a) Inertial-band amplitudes separated into clockwise (solid) and counter-clockwise (dotted) components and averaged from the surface to the second ADCP bin (106 m). (b) Air temperature observed at the IOEB (the sensor could not register temperatures less than –35 C). (c) Eddy-band amplitudes averaged over ADCP depth bins 2–3 (106–154 m). (d) Water depth along the drift track.

Velocity variability in the eddy band was strongest during the first part of the record as the IOEB moved from the northwest Beaufort Sea to the southwest slope of the Canada Basin (Fig. 3c). The eddy-band energy dropped abruptly as the buoy left the basin (day 405). It has been known for some time that eddies populate this region of the Arctic Ocean [*Manley and Hunkins*, 1985], but the IOEB observations are of interest in that they extend the region of observed eddies significantly further south and west in the Canada Basin.

Twenty periods of probable eddy variability, distinguished by sustained subsurface velocity maxima of 10 cm s^{-1} or greater, were observed. The maximum velocities were generally found either in bin 2 (106 m) or 3 (154 m) and ranged from 10–40 cm s^{-1}. Eddy amplitudes were similar in the southeast and southwest Canada Basin, but the number of encounters was greater in the southwest. Approximately three fourths of the velocity anomalies were seen simultaneously in two or three depth bins, implying eddies with vertical extents of 50–150 m. The remainder were seen in only one bin. These basic properties (amplitude, depth of maximum velocity, and vertical extent) are consistent with previous eddy observations in the region [*Manley and Hunkins*, 1985].

The possibility that only the edge of an eddy was encountered, along with vagaries of the drift track, often made it difficult to associate an eddy-like structure with each velocity maximum. Of the 10 most clearly identifiable eddies, all but one showed anticyclonic rotation. A similar predominance of anticyclonic rotation was reported by *Manley and Hunkins* [1985]. No evidence was found of counter-rotating

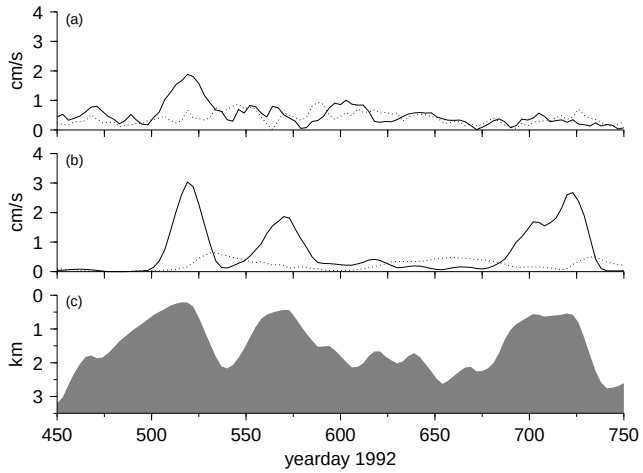

Figure 4. Observed and modeled K_1 tidal amplitude. (a) K_1 amplitude from complex demodulation of ADCP velocities at 154 m separated into clockwise (solid) and counterclockwise (dotted) components. (b) K_1 amplitude from the output of a high-resolution tidal model [*Kowalik and Proshutinsky*, 1993] sampled along the IOEB drift track. (c) Water depth along the drift track.

eddy pairs in the vertical [*D'Asaro*, 1988], although our observations were relatively shallow compared to the likely depth (300–500 m) of the "deep" eddy in a pair.

Amplitudes in the diurnal band were weak during the first half of the record, seldom exceeding the noise level of 0.5 cm s^{-1}. The O_1 and K_1 constituents were of similar amplitude and neither sense of rotation was dominant. The inability to detect a clear signal in the diurnal band was consistent with the weak tides predicted for the Beaufort Sea and Canada Basin. The predicted O_1 tide was small ($\leq$ 0.5 cm s^{-1}) throughout the record, but the predicted K_1 tide increased after day 500 due to interactions with the shallow topography of the Chukchi Shelf and Plateau (Fig. 4). The expectation of an enhanced, clockwise-rotating K_1 tide over the shallow, northward projection of the Chukchi Shelf was borne out in the observations (days 510–530). However, enhancement predicted over the northwest Chukchi Plateau was not observed (days 560–580 and 690–735). The increase in K_1 tidal amplitude beyond that expected from the reduction in depth is due to resonant shelf waves [*Kowalik and Proshutinsky*, 1993]. Small differences between actual and model topography could result in substantial differences in the magnitude and location of this effect.

Acknowledgments. The IOEB deployment was facilitated by the LeadEx Group. The tidal model output was generously provided via the World Wide Web; R. Goldsmith assisted with its analysis. R. Pinkel, G. Gawarkiewicz, and anonymous reviewers provided helpful comments. This work was funded by the Office of Naval Research under Grants N00014-97-1-0135 (AJP) and N00014-92-1-4950 (SH, RK), and by the Japan Marine Science and Technology Center. Woods Hole Oceanographic Institution contribution 9589.

References

Bell, T. H., Topographically generated internal waves in the open ocean, *J. Geophys. Res., 80,* 320–327, 1975.

CEAREX Drift Group, CEAREX drift experiment, *Eos Trans. AGU, 71,* 1115–1118, 1990.

Colony, R. and A. S. Thorndike, An estimate of the mean field of Arctic sea ice motion, *J. Geophys. Res., 89,* 10,623–10,629, 1984.

D'Asaro, E. A., Observations of small eddies in the Beaufort Sea, *J. Geophys. Res., 93,* 6669–6684, 1988.

Honjo, S., T. Takizawa, R. Krishfield, J. Kemp and K. Hatakeyama, Drifting buoys make discoveries about interactive processes in the Arctic Ocean, *Eos Trans. AGU, 76,* 209–219, 1995.

Kowalik, Z. and A. Y. Proshutinsky, Diurnal tides in the Arctic Ocean, *J. Geophys. Res., 98,* 16,449–16,468, 1993.

Kowalik, Z. and A. Y. Proshutinsky, The Arctic ocean tides, in *The Polar Oceans and Their Role in Shaping the Global Environment,* edited by O. M. Johannessen, R. D. Muench and J. E. Overland, pp. 137–157, AGU, Washington, D.C., 1994.

Krishfield, R. K. Doherty and S. Honjo, Ice-Ocean Environmental Buoys (IOEB): Technology and Development in 1991-1992, *Woods Hole Oceanogr. Inst. Tech. Rep. WHOI-93-45*, 138 pp., WHOI, Woods Hole, MA, 1993.

LeadEx Group, The LeadEx experiment, *Eos Trans. AGU, 74,* 393–397, 1993.

Manley, T. O. and K. Hunkins, Mesoscale eddies of the Arctic Ocean, *J. Geophys. Res., 90,* 4911–4930, 1985.

McPhee, M. G., Analysis and prediction of short term ice drift, *J. Offshore Mech. Arctic Eng., 110,* 94–100, 1980a.

McPhee, M. G., An analysis of pack ice drift in summer, in *Sea Ice Processes and Models,*, edited by R. S. Pritchard, pp 62–75, Univ. Wash. Press, Seattle, WA, 1980b.

Pease, C. H., P. Turet and R. S. Pritchard, Barents Sea tidal and inertial motions from Argos ice buoys during the Coordinated Eastern Arctic Experiment *J. Geophys. Res., 100,* 24,705–24,718, 1995.

Pfirman, S. L., R. Colony, D. Nurnberg, H. Eicken and I. Rigor, Reconstructing the origin and trajectory of drifting Arctic sea ice, *J. Geophys. Res., 102,* 12,575–12,586, 1997.

Plueddemann, A. J., A. L. Oien, R. C. Singer and S. P. Smith, *Woods Hole Oceanogr. Inst. Tech. Rep. WHOI-92-05*, 64 pp., WHOI, Woods Hole, MA, 1992.

A. Plueddemann, Dept. of Physical Oceanography, MS-29, Woods Hole Oceanographic Institution, Woods Hole, MA, 02543-1541. (email: aplueddemann@whoi.edu)

S. Honjo and R. Krishfield, Dept. of Geology and Geophysics, MS-23, Woods Hole Oceanographic Institution, Woods Hole, MA, 02543-1541.

T. Takizawa and K. Hatakeyama, Japan Marine Science and Technology Center, 2-15 Natsushima-cho, Yokosuka 237, Japan

(Received September 9, 1997; accepted October 27, 1997.)